

Hardy space infinite elements for time-harmonic two-dimensional elastic waveguide problems*

Martin Halla[†], Lothar Nannen[‡]

October 4, 2018

Abstract

We consider time-harmonic linear elasticity equations in domains containing two-dimensional semi-infinite strips. Since for such problems there exist modes with different signs of group and phase velocity, standard perfectly matched layer (PML) as well as standard Hardy space infinite element methods fail.

We apply a recently developed infinite element method for a physically correct discretization of such waveguide problems which is based on a Laplace transform in propagation direction. In the Laplace domain the space of transformed solutions can be separated into a sum of a space of incoming and a space of outgoing functions where both function spaces are certain Hardy spaces. The Hardy space is chosen such that the construction of a simple infinite element is possible.

The method does not use a modal separation and works on intervals of frequencies. On those intervals the involved operators are frequency independent and hence lead to linear eigenvalue problems when computing resonances. Numerical experiments containing convergence tests and resonance problems are included.

*Support from the Austrian Science Fund (FWF) under grants W1245-N25 and P26252-N25 is acknowledged.

[†]Institute for Analysis and Scientific Computing, Vienna University of Technology, Austria (martin.halla@tuwien.ac.at)

[‡]Institute for Analysis and Scientific Computing, Vienna University of Technology, Austria (lothar.nannen@tuwien.ac.at)

1 Introduction

Computational methods for wave equations bear great attention due to their huge importance for real live problems. In solid mechanics the application reaches from simulating seismic waves, non-destructive testing to material characterization [10, 19]. Such equations are usually posed on unbounded domains Ω . Mesh based methods, i.e. finite difference/volume/element methods deal with that difficulty by truncation of Ω to a bounded subdomain Ω_{int} and special treatment of the exterior domain $\Omega_{\text{ext}} = \Omega \setminus \overline{\Omega_{\text{int}}}$.

Based on representation formulas for the solution in Ω_{ext} with given boundary data at the artificial boundary $\Upsilon = \overline{\Omega_{\text{ext}}} \cap \overline{\Omega_{\text{int}}}$ local approximations of the Dirichlet-to-Neumann operator at Υ can be used (see [11] for a review). Also based on representation formulas for the solution (via a Green function) boundary element methods typically lead to non-local but more accurate approximations.

A method, which does not directly use a representation formula, is the complex scaling method, reintroduced by Bérenger [6] as perfectly matched layer method (PML) for electromagnetic waves. The method became soon very popular and can be classified as today's standard method for treating unbounded domains. In [14] a Hardy space infinite element method (HSIE) was introduced for Helmholtz problems. The method can be understood as a special infinite element method, relying on the pole condition [16]. It features many advantages of PMLs, in particular it does not depend directly on a representation formula. However, the theoretical background of this method is different to that of the PML.

As for all linear wave equations, a fundamental technique in understanding linear elastic wave equations is the study of most simple solutions [12, 2]. In general unbounded domains these are plane waves $e^{i\kappa \cdot \mathbf{x} - i\omega t} \mathbf{w}$, where as in waveguides, such as plates $\mathbb{R}^2 \times I, I \subset \mathbb{R}$ and cylinders $\mathbb{R} \times D, D \subset \mathbb{R}^2$, boundary conditions have to be respected by the solutions. The general form in these cases are modal waves. In semi-infinite cylinders they take the form $e^{i\kappa x - i\omega t} \mathbf{w}(\mathbf{y})$, where $t \in \mathbb{R}_{>0}$ is the time variable, $x \in \mathbb{R}_{>0}$ is the longitudinal coordinate, $\mathbf{y} \in D$ the vector of transverse coordinates, $\omega \in \mathbb{R}_{>0}$ the angular frequency, κ the wavenumber and $\mathbf{w}/|\mathbf{w}|$ the direction of displacement. The frequency ω and the wavenumber κ have to fulfill a wave equation specific dispersion relation $\omega(\kappa)$ to yield a solution. The wave travels in direction $\text{sign}(\kappa)$ with phase velocity ω/κ , whereas the energy is transported in direction $\text{sign}(\partial\omega(\kappa)/\partial\kappa)$ with group velocity $\partial\omega(\kappa)/\partial\kappa$ [21].

The possibility of waves with different signs of group and phase velocity was already discussed by Lamb in 1904 [18]. Such mismatches between the directions of propagation of phase and energy cannot only happen in

waveguides, but also in anisotropic materials [5]. Although PML methods select waves by their propagation direction of phase, the attention to mismatches between propagation directions of phase and energy in elastic materials was omitted for long [5]. This may result in a wrong selection of outgoing/incoming waves and can lead to an exponential growth of solutions in the damping layer of PMLs. Such cases are usually reported as instabilities, due to the definition of stability, but first of all, in such cases an unphysical radiation condition is incorporated in the PML formulation.

Sometimes, such problems can be solved using a transformation of variables [4, 1]. In [29, 22] SMART layers were introduced for seismic waves. They allow more flexibility in the damping than PMLs, but lose the property of being perfectly matched. For semi-infinite linear elastic cylinders in the time-harmonic setting, two methods based on bi-orthogonal relations of modal solutions were proposed: The method presented in [3] is based directly on a modal representation of the solution, whereas in [28, 8] ways to modify standard PMLs are reported. They rely on a smart post processing by exchanging backward incoming with backward outgoing modes. Since, these methods involve modal solutions, which depend non-linearly on ω^2 , they depend themselves non-linearly on ω^2 . Thus if they are used to compute resonances, they lead to non-linear eigenvalue problems. Although solvers for non-linear eigenvalue problems exist (e.g. [7]), they are more involved than solvers for linear eigenvalue problems.

In [13] a new family of Hardy space infinite elements was introduced. It is based on a generalized pole condition, which allows for different signs of phase velocities. The achievement of this paper is to pick up these results and apply it to two-dimensional time-harmonic semi-infinite cylindrical linear elastic waveguide problems. A big advantage of this method is, that ω^2 only enters as a scalar coefficient in the method. Hence, the discretization of a resonance problem leads to a generalized linear matrix eigenvalue problem, which can be treated with a standard solver. Moreover, the numerical results indicate a super-algebraic convergence with respect to the number of degrees of freedom in the longitudinal direction.

The outline of the paper is as follows: Section 2 formulates the diffraction problem to solve, in particular the modal radiation condition and its reformulation as a pole condition. In Section 3 we introduce the Hardy space infinite element in one dimension as in [13] and discuss the choice of method parameters for the investigated elasticity problem. Section 4 explains the discretization of the elasticity problem with the use of tensor product basis functions. Section 5 deals with the spectral objects and properties of resonance problems. Finally, in Section 6 we give numerical examples.

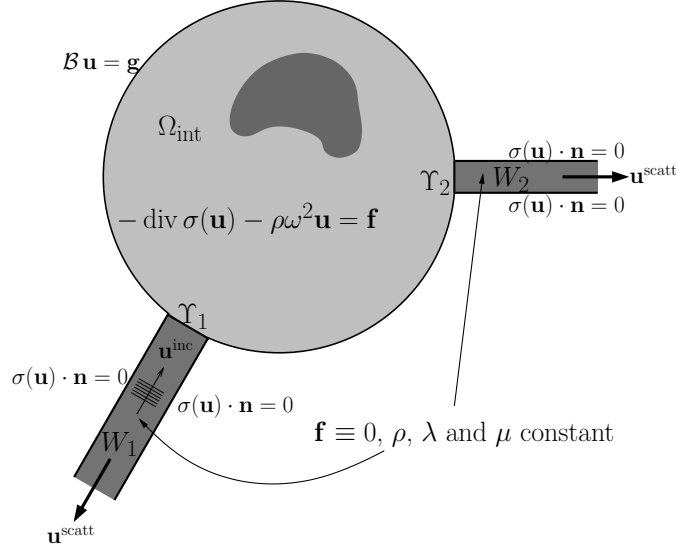


Figure 1: sketch of an elastic waveguide problem under consideration in this paper

2 General setting

2.1 Geometry and elasticity Equations

We are considering in this paper elastic waveguide problems in two dimensions (see Fig. 1 for a typical situation): The domain of interest Ω consists of a bounded interior domain Ω_{int} and L semi-infinite waveguides W_1, \dots, W_L with interfaces $\Upsilon_1, \dots, \Upsilon_L$. The two-dimensional time-harmonic isotropic linear elasticity problem is given by

$$-\text{div } \boldsymbol{\sigma}(\mathbf{u}) - \rho\omega^2\mathbf{u} = \mathbf{f} \text{ in } \Omega, \quad (2.1a)$$

$$\mathcal{B}\mathbf{u} = \mathbf{g} \text{ on } \partial\Omega, \quad (2.1b)$$

$$\mathbf{u} - \mathbf{u}^{\text{inc}} \text{ satisfies a radiation condition in each waveguide } W_\ell, \quad \ell = 1, \dots, L. \quad (2.1c)$$

Here, $\Re(\mathbf{u}(\mathbf{x})e^{-i\omega t})$ for $\mathbf{x} \in \Omega$ and time $t > 0$ is the time-harmonic displacement vector, $\rho > 0$ the density, $\omega > 0$ the angular frequency, $\lambda, \mu > 0$ are Lamé parameters, $\boldsymbol{\epsilon}(\mathbf{u}) = \frac{1}{2}(\nabla\mathbf{u} + (\nabla\mathbf{u})^\top)$ the strain tensor, $\boldsymbol{\sigma}(\mathbf{u}) = \lambda \text{div } \mathbf{u} \cdot \mathbf{Id} + 2\mu\boldsymbol{\epsilon}(\mathbf{u})$ the stress tensor, and \mathbf{f} a volumetric force. In this paper we will always use the plain strain model (see e.g. [9]), i.e. the Lamé parameters are related to Young's modulus E and Poisson's ratio ν by $\mu = \frac{E}{2(1+\nu)}$ and $\lambda = \frac{E\nu}{(1+\nu)(1-2\nu)}$. Boundary conditions at $\partial\Omega_{\text{int}} \cap \partial\Omega$ are formulated in

terms of a trace operator \mathcal{B} , e.g. a Dirichlet trace operator $\mathcal{B}\mathbf{u} = \mathbf{u}$ or a Neumann trace operator $\mathcal{B}\mathbf{u} = \sigma(\mathbf{u}) \cdot \mathbf{n}$ with outer normal vector \mathbf{n} , and a boundary datum \mathbf{g} .

We will assume in the following, that ρ , λ and μ are constant in each waveguide W_ℓ , that there exists no volumetric force \mathbf{f} in the waveguides, and that we have traction free boundary conditions $\sigma(\mathbf{u}) \cdot \mathbf{n} = 0$ at the boundaries $\partial W_\ell \cap \partial\Omega$. The terms radiation condition and incident field \mathbf{u}^{inc} in (2.1c) and in Fig. 1 will become clear in the next subsection.

In addition to the scattering problem (2.1), where the angular frequency ω and the sources \mathbf{f} , \mathbf{g} , and \mathbf{u}^{inc} are given, we will consider the corresponding resonance problem: Find resonances $\omega \in \mathbb{C}$ with positive real part and non-trivial resonance functions \mathbf{u} such that

$$-\operatorname{div} \sigma(\mathbf{u}) - \rho\omega^2 \mathbf{u} = \mathbf{0} \text{ in } \Omega, \quad (2.2a)$$

$$\mathcal{B}\mathbf{u} = \mathbf{0} \text{ on } \partial\Omega, \quad (2.2b)$$

$$\mathbf{u} \text{ satisfies a radiation condition in each waveguide } W_\ell, \quad \ell = 1, \dots, L. \quad (2.2c)$$

2.2 Radiation condition

In order to define a physically correct radiation condition (2.1c), we consider in this section one single waveguide. The generalization to multiple waveguides is straightforward. Let $W := \mathbb{R}^+ \times (-R, R)$ be a reference waveguide and ρ , λ and μ be constant and positive. As for most other problems the radiation condition can be derived by an analytic representation of solutions. For waveguides a convenient representation is a modal sum. For given angular frequency $\omega > 0$ we call $\mathbf{u}(\bullet, \bullet; \omega)$ a mode with wavenumber $\kappa(\omega) \in \mathbb{C}$, if it has the form

$$\mathbf{u}(\xi, \eta; \omega) = e^{i\kappa(\omega)\xi} \mathbf{w}(\eta; \omega), \quad (\xi, \eta) \in W, \omega \in \mathbb{R}^+, \quad (2.3)$$

and solves

$$-\operatorname{div} \sigma(\mathbf{u}) - \rho\omega^2 \mathbf{u} = 0, \quad (\xi, \eta) \in W, \quad (2.4a)$$

$$\sigma(\mathbf{u}) \cdot \begin{pmatrix} 0 \\ 1 \end{pmatrix} = 0, \quad (\xi, \eta) \in \mathbb{R}_+ \times \{-R, R\}. \quad (2.4b)$$

It is straightforward to see that if $e^{i\kappa(\omega)\xi} \begin{pmatrix} \mathbf{w}_1(\eta; \omega) \\ \mathbf{w}_2(\eta; \omega) \end{pmatrix}$ is a mode, so is $e^{-i\kappa(\omega)\xi} \begin{pmatrix} \mathbf{w}_1(\eta; \omega) \\ -\mathbf{w}_2(\eta; \omega) \end{pmatrix}$ as well as $e^{-i\bar{\kappa}(\omega)\xi} \begin{pmatrix} \bar{\mathbf{w}}_1(\eta; \omega) \\ \bar{\mathbf{w}}_2(\eta; \omega) \end{pmatrix}$ and $e^{i\bar{\kappa}(\omega)\xi} \begin{pmatrix} \bar{\mathbf{w}}_1(\eta; \omega) \\ -\bar{\mathbf{w}}_2(\eta; \omega) \end{pmatrix}$. A physical solution should be bounded for $\xi \rightarrow \infty$. Hence, if $\Im(\kappa(\omega)) \neq 0$ we want to exclude modes

with $\Im(\kappa(\omega)) < 0$. In this case, we call the exponentially decaying modes *evanescent*. If $\Im(\kappa(\omega)) = 0$, both modes with wavenumbers $\pm\kappa(\omega)$ stay bounded and it is not obvious which one is physically relevant. We give here two approaches leading to the same distinguishing criterion. For both we assume, that $\Re(\partial_\omega\kappa(\omega)) \neq 0$, $\Im(\partial_\omega\kappa(\omega)) = 0$.

1. [21] states that the velocity of energy transport of a mode is given by the group velocity $\partial\omega(\kappa)/\partial\kappa$ which has the same sign as $\partial\kappa(\omega)/\partial\omega$. Since in problem (2.4) there is no source in W , energy should be radiated to infinity and therefore $\partial\kappa(\omega)/\partial\omega > 0$. See also [17, Rem. 3.1].
2. For the *limiting absorption principle* we add an artificial small damping $\epsilon > 0$ to the system, i.e. we substitute $\omega > 0$ by $\omega + i\epsilon$. The corresponding solution \mathbf{u}_ϵ to the damped version of (2.4) should be bounded for $x \rightarrow \infty$. Since by linearization $|\exp(i\kappa(\omega + i\epsilon)\xi)| \approx \exp\left(-\frac{\partial\kappa(\omega)}{\partial\omega}\xi\right)$ this leads to $\partial\kappa(\omega)/\partial\omega > 0$. For further details see [17, Cor. 3.1].

Therefore, if $\partial\kappa(\omega)/\partial\omega > 0$ we call $e^{i\kappa(\omega)\xi} \begin{pmatrix} \mathbf{w}_1(\eta;\omega) \\ \mathbf{w}_2(\eta;\omega) \end{pmatrix}$ an *outward propagating mode* and $e^{-i\kappa(\omega)\xi} \begin{pmatrix} \mathbf{w}_1(\eta;\omega) \\ -\mathbf{w}_2(\eta;\omega) \end{pmatrix}$ an *inward propagating mode*. Note, that there exist modes with different signs of phase and group velocity (see Fig. 2). We call a wavenumber $\kappa(\omega)$ *outgoing*, if there exists an evanescent or outward propagating mode of the form (2.3) satisfying (2.4). In other words $\kappa(\omega)$ is outgoing (*incoming*), if

1. $\partial_\omega\kappa(\omega) > 0$ ($\partial_\omega\kappa(\omega) < 0$) for real wavenumbers $\kappa(\omega) \in \mathbb{R}$, and
2. $\Im(\kappa(\omega)) > 0$ ($\Im(\kappa(\omega)) < 0$) for non-real wavenumbers $\kappa(\omega) \notin \mathbb{R}$.

A function satisfies the radiation condition in the waveguide W and is called *outgoing*, if it can be approximated by a linear combination of evanescent and outward propagating modes. It is not a priori clear, that the traces of evanescent and outward propagating modes on the waveguide interface $\Upsilon = \{0\} \times (-R, R)$ are dense in $L^2(\Upsilon)^2$. In the following Remark we cite some results from [17], which justify our definition of the radiation condition.

Remark 2.1 *In [17] a rigorous analysis of modal decompositions for two and three dimensional elastic waveguides is given using a quadratic eigenvalue problem. There, not only modes (eigenfunctions) of the form (2.3) are considered, but also the generalized eigenspaces of the investigated quadratic eigenvalue problem (see [17, (0.10)]). We refer to these functions of the generalized eigenspace, which are not eigenfunctions, as associated modes in this paper. We briefly summarize the main results of [17]:*

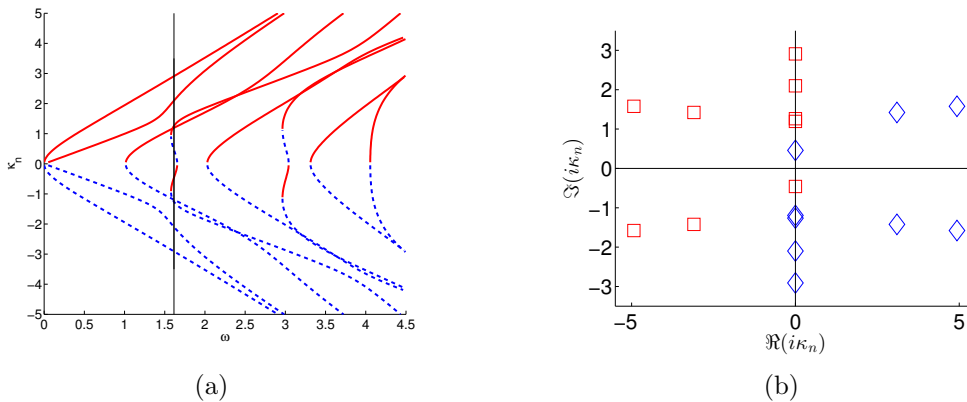


Figure 2: left: the first eight dispersion curves. Modes corresponding to the red solid part have positive group velocity and modes corresponding to the blue dashed part have negative group velocity. right: the first nine outgoing/incoming wavenumbers multiplied with i marked with red squares/blue diamonds at frequency $\omega = 1.615$. Parameters are $H = \rho = E = 1$, and $\nu = 0.2$.

1. [17, Thm. 1.5]: For fixed $\omega > 0$ there exist wavenumbers $\kappa_n(\omega), n \in \mathbb{N}$, symmetrically situated relative to the real axis and the origin. They are situated in arbitrarily small angles, adjoining the imaginary axis, with the exception of a finite number of wavenumbers. In particular, only a finite number $\kappa_n(\omega) \in \mathbb{R}$ exists.
2. [17, Thm. 3.8]: There exists a sequence of frequencies $0 = \omega_1^2 < \omega_2^2 < \dots < \omega_n^2 \rightarrow \infty$, such that for all $\omega \in \mathbb{R}^+ \setminus \{\omega_n, n \in \mathbb{N}\}$ the implication $\kappa_n(\omega) \in \mathbb{R} \Rightarrow \partial_\omega \kappa_n(\omega) \in \mathbb{R} \setminus \{0\}$ holds.
3. [17, Thm. 2.5]: Assume $\omega \in \mathbb{R}^+ \setminus \{\omega_n, n \in \mathbb{N}\}$. Then the traces of modes and associated modes corresponding to $\{\kappa_n(\omega), n \in \mathbb{N} : \Im(\kappa_n(\omega)) > 0 \vee (\kappa_n(\omega) \in \mathbb{R} \wedge \partial_\omega \kappa_n(\omega) > 0)\}$ are dense and minimal in $L^2(\Upsilon)^2$ as well as in $H^1(\Upsilon)^2$.

2.3 Numerical implementations of the radiation condition

In a numerical method for (2.1) the radiation condition as to be taken into account. Due to the simple waveguide geometry, methods based on modal decompositions as the one proposed in [3] are popular. Assuming that every so-

lution in a waveguide can be expanded in a sum of modes $\sum_{n \in \mathbb{N}} e^{i\kappa_n(\omega)\xi} \mathbf{w}_n(\eta)$, a Dirichlet-to-Neumann operator can be defined as

$$\text{DtN} \sum_{n \in \mathbb{N}} e^{i\kappa_n(\omega)\xi} \mathbf{w}_n(\eta) := \sum_{n \in \mathbb{N}} \sigma_n(e^{i\kappa_n(\omega)\xi} \mathbf{w}_n(\eta)). \quad (2.5)$$

Truncating the waveguides W_l and posing $\sigma_n(\mathbf{u}) = \text{DtN} \mathbf{u}$ at the artificial ends leads to a formulation of (2.1) in a bounded domain. For a numerical method standard finite element methods for the bounded domain can be used together with a discrete Dirichlet-to-Neumann operator $(\text{DtN})_N$, which can be constructed by using only a finite number of modes in (2.5), i.e. $(\text{DtN})_N \sum_{n \leq N} e^{i\kappa_n(\omega)\xi} \mathbf{w}_n(\eta) := \sum_{n \leq N} \sigma_n(e^{i\kappa_n(\omega)\xi} \mathbf{w}_n(\eta))$. It can be shown that the modes satisfy biorthogonal relations, which can be exploited to implement $(\text{DtN})_N$ in an elegant way, as done in [3]. However, the method requires a precomputation of the modes. Moreover, since the modes depend on ω , the discretization matrix will depend non-linearly on ω . Hence, discretizing the resonance problem (2.2) leads to a large, non-linear eigenvalue problem.

In [20] a numerical method for a Helmholtz problem is proposed based on eigenfunction expansions of the bounded interior problem coupled to mode expansions in the waveguides. These approaches lead again to non-linear, but comparatively small eigenvalue problems. Nevertheless, solving the non-linear eigenvalue problem numerically is a non-trivial task and of course a computation of the modes and interior eigenfunctions is needed.

A popular method which does not depend on the computation of the modes is the perfectly matched layer method. The longitudinal direction ξ of the waveguide is thereby complex scaled by $\alpha \in \mathbb{C}$, i.e. $\tilde{\xi} := \alpha\xi$, leading to a new equation for $\tilde{\mathbf{u}}(\xi, \eta) := \mathbf{u}(\tilde{\xi}, \eta)$. If α is chosen such that $\Re(\alpha i\kappa_n(\omega)) < 0$ for all outgoing wavenumbers $\kappa_n(\omega)$ and \mathbf{u} is an outgoing solution of the original problem, then $\tilde{\mathbf{u}}$ is exponentially decaying in ξ . Hence, a truncation of the infinite waveguide to a finite waveguide with zero Neumann or Dirichlet boundary condition at the end introduces only a small error due to the exponential decay. The resulting equation can then be discretized with standard methods, as it is posed on a finite domain. The linear system matrix takes the form $K_h - \omega^2 M_h$. When looking for resonances, the above leads to generalized linear matrix eigenvalue problems, which is a main advantage in view of numerical algorithms.

The reason why perfectly matched layers are only of limited use for waveguide problems with backward propagating modes, is that no $\alpha \in \mathbb{C}$ can exist, such that $\Re(\alpha i\kappa_n(\omega)) < 0$ for all outgoing wavenumbers $\kappa_n(\omega)$ (see Fig. 2(b), a multiplication with α leads to a rotation of $i\kappa_n$ in the complex plane). The modified perfectly matched layer methods presented in [28, 8] combine

complex scaling with a special treatment of the backward propagating mode. For scattering problems with only a few backward propagating modes this approach works well, but again it leads to non-linear eigenvalue problems when discretizing the resonance problem (2.2).

2.4 Pole Condition

Our goal is to construct a radiation condition, which combines the advantages of the methods presented in the previous subsection: It should yield physically correct solutions and discretizations of resonance problems should lead to linear matrix eigenvalue problems. Again for the sake of simplicity, we formulate the following only for the reference waveguide W . For $\omega > 0$ let

$$\mathbf{u}(\xi, \eta) = \sum_n^N c_n \mathbf{u}_n(\xi, \eta), \quad (\xi, \eta) \in W,$$

with $c_n \in \mathbb{C}$ be a finite sum of modes and associated modes with outgoing wavenumbers $\kappa_n(\omega) \in \mathbb{C}$. Then \mathbf{u} is bounded and the Laplace transform in the longitudinal direction $\mathcal{L}(\mathbf{u}(\bullet, \eta))(s)$ for $(s, \eta) \in \mathbb{R}_+ \times (-R, R)$ takes the form

$$\mathcal{L}(\mathbf{u}(\bullet, \eta))(s) = \sum_n^N \frac{c_n}{(s - \mathbf{i}\kappa_n)^{m_n}} \tilde{\mathbf{w}}_n(\eta), \quad (2.6)$$

with $m_n \in \mathbb{N}$. It has a meromorphic extension to \mathbb{C} with poles at $\{\mathbf{i}\kappa_n\}$. In contrast, the Laplace transform of $e^{-\mathbf{i}\kappa_n \xi}$ has a pole at $-\mathbf{i}\kappa_n$ (see Fig. 2(b) for a typical situation). The *pole condition* states, that \mathbf{u} is called outgoing, if $\mathcal{L} \mathbf{u}$ has no poles in a suitable region of the complex plane. Here, one might chose a point symmetric, smooth and asymptotically straight boundary curve Γ separating the outgoing from the incoming poles, simply connected domains Γ^- , Γ^+ such that $\mathbb{C} = \Gamma^- \dot{\cup} \Gamma \dot{\cup} \Gamma^+$ and asks $\mathcal{L} \mathbf{u}$ to be holomorphic in Γ^- . Typical choices of Γ can be seen in Fig. 4. The assumption

$$\mathbb{S}(\omega) \subset \Gamma^+, \quad (2.7)$$

with $\mathbb{S}(\omega) := \{\mathbf{i}\kappa_1(\omega), \mathbf{i}\kappa_2(\omega), \dots\}$ being the set of outgoing wavenumbers multiplied with \mathbf{i} for the frequency ω , is thereby essential. To formulate the above in a more compact way, we introduce the *Hardy space* $H^-(\Gamma)$ as the subspace of $L^2(\Gamma)$, such that for each $f \in H^-(\Gamma)$ there exists an in Γ^- holomorphic function f_{vol} with f being the non-tangential limit of f_{vol} . We refer to [13, App. A] for a detailed definition and properties of such Hardy

spaces. We can formulate the pole condition now in the following way

$$\mathcal{L} \mathbf{u} \in [H^-(\Gamma) \otimes L^2(\tilde{\Upsilon})]^2. \quad (2.8)$$

If (2.7) holds true, then the modal radiation condition of Sec. 2.2 is equivalent to the pole condition (2.8) for solutions \mathbf{u} to Equ. (2.4) having the form $\mathbf{u} = \sum_{n=1}^N c_n \mathbf{u}_n$ and \mathbf{u}_n being modes and associated modes.

The pole condition (2.8) does not depend on the wavenumbers but only on Γ and is therefore frequency independent. The wavenumbers are hidden in the assumption (2.7). Of course, we have to discuss how to chose Γ (see Sec. 3.3). Moreover, for the interpretation of solutions to the resonance problem (2.2) in Sec. 5 we need the wavenumbers. But the numerical method based on (2.8) presented in the following sections is independent of the wavenumbers and waveguide modes. This facilitates the implementation of the method a lot. Moreover, a discretization of the resonance problem (2.2) leads to a linear generalized matrix eigenvalue problem.

3 The Hardy space infinite element

The pole condition $\mathcal{L} \mathbf{u} \in [H^-(\Gamma) \otimes L^2(\tilde{\Upsilon})]^2$ is a nice way to reformulate the physical radiation condition, but a stable numerical method based on this framework is delicate. In [13] such a method was developed for a one dimensional toy problem including a complete convergence analysis. We present here only the results needed for an implementation in the setting of a convected one dimensional Helmholtz equation

$$-u'' + u' - \omega^2 u = 0, \quad x > 0, \quad (3.1a)$$

$$u'(0) = u'_0, \quad (3.1b)$$

$$\mathcal{L} u \in H^-(\Gamma), \quad (3.1c)$$

whereas the curve Γ is chosen such that the solution to (3.1) is unique. Since solutions of (3.1a) have the form $C_1 e^{i\kappa_1 x} + C_2 e^{i\kappa_2 x}$ with $C_1, C_2, \kappa_1, \kappa_2 \in \mathbb{C}$, the curve Γ is such that $i\kappa_1 \in \Gamma^+$ and $i\kappa_2 \in \Gamma^-$ (or vice-versa).

The discretization of the elasticity problem discussed in Section 4 will be straightforward. In order to enhance readability, we have refrained from giving the correct mathematical framework including the variational formulation in the Hardy space. For the elastic waveguide problem this can be deduced along the lines of [13] and [15].

3.1 Basis functions and infinite element matrices

Similar to a classical infinite element method we start with the variational form

$$\int_0^\infty u'v \, dx' + \int_0^\infty u'v \, dx - \omega^2 \int_0^\infty uv \, dx = -u'_0v(0) \quad (3.2)$$

of (3.1), which holds true for the solution u and sufficiently fast decaying, smooth test functions v . We are using a Galerkin scheme with the same basis functions φ_j^{long} , $j \in \mathbb{N}$, as ansatz and test functions. These basis functions should fulfill the pole condition $\mathcal{L} \varphi_j^{\text{long}} \in H^-(\Gamma)$.

From [13] we know that for any two complex parameters $s_0, s_1 \in \Gamma_+$ the linear hull of

$$\psi_j^{s_0, s_1}(s) := \frac{s_0 + s_1}{s - s_1} \left(\frac{s + s_0}{s - s_0} \right)^{\lfloor (j+1)/2 \rfloor} \left(\frac{s + s_1}{s - s_1} \right)^{\lfloor j/2 \rfloor}, \quad j \in \mathbb{N}_0, \quad (3.3)$$

is dense in the Hardy space $H^-(\Gamma)$. The basis functions φ_j^{long} of our Galerkin scheme are defined via their Laplace transforms

$$(\mathcal{L} \varphi_1^{\text{long}})(s) := \frac{1}{s - s_0}, \quad (\mathcal{L} \varphi_j^{\text{long}})(s) := \frac{\psi_{j-2}^{s_0, s_1}(s)}{s - s_0}, \quad j = 2, \dots, \quad s \in \Gamma. \quad (3.4)$$

They have the form

$$\varphi_j^{\text{long}}(x) = e^{s_0 x} p_j^{s_0}(x) + e^{s_1 x} p_j^{s_1}(x), \quad x \geq 0,$$

with polynomials $p_j^{s_0}, p_j^{s_1}$ and in particular $\text{span}\{\varphi_0^{\text{long}}, \varphi_1^{\text{long}}\} = \text{span}\{e^{s_0 x}, e^{s_1 x}\}$. Comparing the basis functions with the modes (2.3) shows, that these functions represent the longitudinal part of the modes exactly for wavenumbers $\kappa = s_0/i$ and $\kappa = s_1/i$. Therefore, s_0/i and s_1/i can be considered as two different wavenumbers. The actual choice of these parameters will be discussed in the next subsections.

It is easy to show that φ_j^{long} , $j \in \mathbb{N}$ fulfill the pole condition and moreover, by a limit theorem of the Laplace transform there holds

$$\varphi_j^{\text{long}}(0) = \lim_{x \searrow 0} \varphi_j^{\text{long}}(x) = \lim_{s \rightarrow \infty} s(\mathcal{L} \varphi_j^{\text{long}})(s) = \begin{cases} 1, & j = 1 \\ 0, & j > 1 \end{cases}.$$

This facilitates coupling of these basis functions at $x = 0$ with e.g. standard finite element basis functions for $x < 0$.

We are left with the computation of the integrals in (3.2) using φ_j^{long} for u and v . If s_0 and s_1 are chosen with negative real part, the integrals are

bounded. Similar to [14, Lemma A.1] it can be shown, that

$$\int_0^\infty \varphi_j^{\text{long}}(x)\varphi_k^{\text{long}}(x) dx = \frac{-i}{2\pi} \int_\Gamma (\mathcal{L}\varphi_j^{\text{long}})(s)(\mathcal{L}\varphi_k^{\text{long}})(-s), ds, \quad j, k \in \mathbb{N}. \quad (3.5)$$

Since $\mathcal{L}\varphi_j^{\text{long}}$ are meromorphic functions, the integrals on the right hand side can be computed by the residue theorem. Following the computations in [13], the infinite mass matrix $(M_{\text{long}}^\infty)_{j,k} := \int_0^\infty \varphi_j^{\text{long}}(x)\varphi_k^{\text{long}}(x) dx$ is given by the tridiagonal matrix

$$M_{\text{long}}^\infty = \frac{-1}{s_0 s_1} \begin{pmatrix} \boxed{\begin{matrix} s_1 & -s_1 \\ -s_1 & s_0+s_1 \end{matrix}} & \boxed{\begin{matrix} 0 & 0 \\ -s_0 & 0 \end{matrix}} & & \\ \boxed{\begin{matrix} 0 & -s_0 \\ 0 & 0 \end{matrix}} & \boxed{\begin{matrix} s_0+s_1 & -s_1 \\ -s_1 & s_0+s_1 \end{matrix}} & \ddots & \\ & & \ddots & \ddots \end{pmatrix}. \quad (3.6)$$

Analogue calculations can be performed for $\partial_x \varphi_j^{\text{long}}$, since

$$(\mathcal{L}\partial_x \varphi_1^{\text{long}})(s) = \frac{s_0}{s-s_0}, \quad (\mathcal{L}\partial_x \varphi_j^{\text{long}})(s) = \frac{s\psi_{j-2}^{s_0, s_1}(s)}{s-s_0}, \quad j = 2, \dots$$

The drift $(D_{\text{long}}^\infty)_{jk} := \int_0^\infty \partial_x \varphi_j^{\text{long}}(x)\varphi_k^{\text{long}}(x) dx$ and stiffness $(S_{\text{long}}^\infty)_{jk} := \int_0^\infty \partial_x \varphi_j^{\text{long}}(x)\partial_x \varphi_k^{\text{long}}(x) dx$ matrices are given by

$$D_{\text{long}}^\infty = \frac{1}{2} \begin{pmatrix} 1 & 1 & & \\ -1 & 0 & 1 & \\ & -1 & 0 & \ddots \\ & & \ddots & \ddots \end{pmatrix}, \quad S_{\text{long}}^\infty = \frac{-1}{2} \begin{pmatrix} \boxed{\begin{matrix} s_0 & s_0 \\ s_0 & s_0+s_1 \end{matrix}} & \boxed{\begin{matrix} 0 & 0 \\ s_1 & 0 \end{matrix}} & & \\ \boxed{\begin{matrix} 0 & s_1 \\ 0 & 0 \end{matrix}} & \boxed{\begin{matrix} s_0+s_1 & s_0 \\ s_0 & s_0+s_1 \end{matrix}} & \ddots & \\ & & \ddots & \ddots \end{pmatrix}. \quad (3.7)$$

Using only the first N^{long} basis functions and therefore only the $N^{\text{long}} \times N^{\text{long}}$ upper left block of these matrices leads to the discretization of (3.2): Find $U^{(N^{\text{long}})} \in \mathbb{C}^{N^{\text{long}}}$ such that

$$\left(S_{\text{long}}^{N^{\text{long}}} + D_{\text{long}}^{N^{\text{long}}} - \omega^2 M_{\text{long}}^{N^{\text{long}}} \right) U^{(N^{\text{long}})} = (-u'_0, 0, \dots, 0)^\top. \quad (3.8)$$

Note, that the matrices $S_{\text{long}}^{N^{\text{long}}}$, $D_{\text{long}}^{N^{\text{long}}}$ and $M_{\text{long}}^{N^{\text{long}}}$ are independent of the angular frequency ω .

3.2 Relation between the method parameters s_0 , s_1 and Γ

(3.8) is a conforming discretization of (3.1a)-(3.1b). The side constraint $\mathcal{L}\sum_{j=1}^{N^{\text{long}}} U_j^{(N^{\text{long}})}\varphi_j^{\text{long}} \in H^-(\Gamma)$ (see (3.1c)) is however not only fulfilled for

the chosen Γ , but for any $\tilde{\Gamma}$ with $s_0, s_1 \in \tilde{\Gamma}^+$. If for such a second $\tilde{\Gamma}$ the wavenumbers $\kappa_{1,2}$ of (3.1a) multiplied with \mathbf{i} belong to different sides of the curves, e.g. $\mathbf{i}\kappa_1 \in \Gamma^+ \cap \tilde{\Gamma}^-$ and $\mathbf{i}\kappa_2 \in \Gamma^- \cap \tilde{\Gamma}^+$, Equations (3.1a)-(3.1b) together with the condition $\mathcal{L}u \in H^-(\tilde{\Gamma})$ define a different solution than (3.1). But (3.8) is again a conforming discretization for this second problem. This leads to the question that if the solutions $\sum_{j=1}^{N^{\text{long}}} U_j^{(N^{\text{long}})} \varphi_j^{\text{long}}$ of (3.8) converge (in any norm) to a function U , does $\mathcal{L}U \in H^-(\Gamma)$ or $\mathcal{L}U \in H^-(\tilde{\Gamma})$ hold?

The answer was given in [13]: The linear hull of the functions $\mathcal{L}\varphi_j^{\text{long}}$, $j \in \mathbb{N}$, is dense in any $H^-(\Gamma)$ with $s_0, s_1 \in \Gamma^+$. But they form a stable basis only in one specific space $H^-(\Gamma_{s_0, s_1})$, i.e. any $U \in H^-(\Gamma_{s_0, s_1})$ can be expanded $U = \sum_{j \in \mathbb{N}} \alpha_j \mathcal{L}\varphi_j^{\text{long}}$ with a square summable sequence $(\alpha_j)_{j \in \mathbb{N}}$. One can deduce that if $\{\mathbf{i}\kappa_1, \mathbf{i}\kappa_2\} \cap \Gamma^\pm = \{\mathbf{i}\kappa_1, \mathbf{i}\kappa_2\} \cap \Gamma_{s_0, s_1}^\pm$ Eq. (3.8) is uniquely solvable at least for sufficiently large N^{long} with solutions $U^{(N^{\text{long}})}$ and $\lim_{N^{\text{long}} \rightarrow \infty} \|\mathcal{L}u - \sum_{j=1}^{N^{\text{long}}} U_j^{(N^{\text{long}})} \mathcal{L}\varphi_j^{\text{long}}\|_{L^2(\Gamma_{s_0, s_1})} = 0$ holds. Thence the choice of s_0, s_1 for (3.8) implicitly poses the pole condition w.r.t. Γ_{s_0, s_1} on the solution u of (3.1).

The curve Γ_{s_0, s_1} is given by the algebraic variety

$$\Gamma_{s_0, s_1} := \left\{ s \in \mathbb{C} : \left| \frac{s + s_0}{s - s_0} \frac{s + s_1}{s - s_1} \right| = 1 \right\}. \quad (3.9)$$

In order to have a physically correct pole condition for elastic waveguide problems we are left with the task to find s_0, s_1 such that $\mathbb{S}(\omega) \subset \Gamma_{s_0, s_1}^+$, which will be the issue of the next subsection. The following properties of the curve Γ_{s_0, s_1} can all be deduced from (3.9): First of all for $g_{s_0, s_1}(s) := \frac{|s - s_0| |s - s_1|}{|s + s_0| |s + s_1|}$ we have the characterizations

$$\Gamma_{s_0, s_1}^+ = \{s \in \mathbb{C} : g_{s_0, s_1}(s) < 1\}, \quad \Gamma_{s_0, s_1} = \{s \in \mathbb{C} : g_{s_0, s_1}(s) = 1\}, \quad \text{and} \quad \Gamma_{s_0, s_1}^- = \{s \in \mathbb{C} : g_{s_0, s_1}(s) > 1\}. \quad (3.10)$$

The curve can explicitly be parameterized by $\Gamma_{s_0, s_1} = \gamma_{s_0, s_1}(\mathbb{R})$ with

$$\gamma_{s_0, s_1}(r) := -\mathbf{i}r \frac{r^2(s_0 + s_1) + |s_0|^2 s_1 + |s_1|^2 s_0}{|r^2(s_0 + s_1) + |s_0|^2 s_1 + |s_1|^2 s_0|}, \quad r \in \mathbb{R}, \quad (3.11)$$

which shows that its asymptotic behavior is a line. In the case $|s_0| = |s_1|$ it actually is a line. Further scaling the poles scales the curve: $\Gamma_{rs_0, rs_1} = r\Gamma_{s_0, s_1}$ for all $r > 0$. If we chose s_0, s_1 such that

$$\Re(s_0), \Re(s_1) < 0, \quad (3.12a)$$

$$\Im(s_0 + s_1) > 0, \quad (3.12b)$$

$$|s_0|^2 \Im(s_1) + |s_1|^2 \Im(s_0) < 0, \quad (3.12c)$$

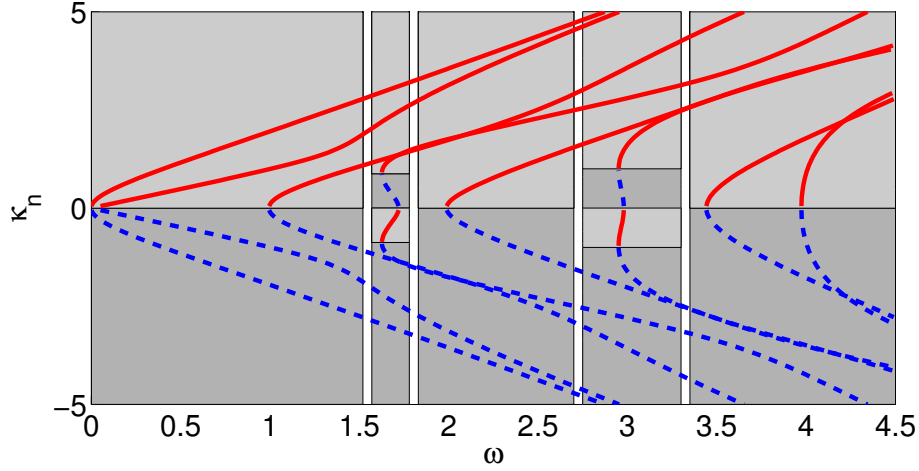


Figure 3: The first eight dispersion curves for $H = \rho = E = 1$ and $\nu = 0.25$. Modes corresponding to the red solid part have positive group velocity and modes corresponding to the blue dashed part have negative group velocity.

it holds $i(-\zeta(s_0, s_1), 0) \cup i(\zeta(s_0, s_1), \infty) \subset \Gamma_{s_0, s_1}^+$ and $i(0, \zeta(s_0, s_1)) \cup i(-\infty, -\zeta(s_0, s_1)) \subset \Gamma_{s_0, s_1}^-$ with

$$\zeta(s_0, s_1) := \sqrt{-\frac{|s_0|^2 \Im(s_1) + |s_1|^2 \Im(s_0)}{\Im(s_0 + s_1)}}. \quad (3.13)$$

3.3 Choice of s_0 and s_1

Coming back to the elastic waveguide problem, we inspect the location and qualitative properties of the wavenumber spectrum in order to find reasonable values for the parameters s_0 and s_1 . First, let us look only on the real wavenumbers in Fig. 3 for fixed parameters ν and H, ρ, E . There exist eight frequencies $\omega > 0$ which support waves with vanishing group velocities $(\frac{\partial \kappa_n}{\partial \omega})^{-1}$. Six of them yield vanishing wavenumbers $\kappa_n(\omega) = 0$ and two don't. These 8 frequencies $\omega_1, \dots, \omega_8$ are part of the sequence of frequencies defined in Rem. 2.1 and cannot be treated by the pole condition, since for $\omega \rightarrow \omega_j$ for $j = 1, \dots, 8$ an outgoing wavenumber converges to an incoming wavenumber. Hence, outgoing wavenumbers cannot be separated by Γ from incoming wavenumbers. In Fig. 3 we have made a (non unique) decomposition into five intervals (a, b) such that for all $\omega \in (a, b) \setminus \{\omega_1, \dots, \omega_8\}$ one of the two following cases hold true:

1. For all real wavenumbers the signs of group velocity and phase velocity coincide. Hence, the real wavenumbers with positive group velocity belong to $(0, \infty)$.
2. There exists $\theta > 0$, such that the real wavenumbers with positive group velocity belong to $(-\theta, 0) \cup (\theta, \infty)$.

Hence, the first case requires $\mathbf{i}(0, \infty) \subset \Gamma^+$ and the second case $\mathbf{i}(-\theta, 0) \cup \mathbf{i}(\theta, \infty) \subset \Gamma^+$. Choosing different parameters H, ρ, E would only result in a different scaling of Fig. 3. On the other hand varying ν changes the qualitative behavior. Nevertheless, for all ω either the first case or the second case seems to be true for cylindrical elastic waveguide problems with constant E, ρ , and ν in the waveguides (at least the authors were not able to find any contradicting parameters).

For the non-real outgoing wavenumbers it is known (see Rem 2.1), that for a fixed frequency they are contained in a circular proper subsector of $\{s \in \mathbb{C}: \Im s > 0\}$. Because the wavenumbers are continuous with respect to ω , the above also holds uniformly for ω in suitable small intervals.

For an implementation we have to discuss how to choose the parameters s_0 and s_1 in order to yield $\mathbb{S}(\omega) \subset \Gamma_{s_0, s_1}^+$. For the two cases from above (see Fig. 4) we can proceed as follows:

1. $\mathbf{i}(0, \infty) \subset \Gamma^+$ (Fig. 4(a)): The choice $|s_0| = |s_1|$ is sufficient. In particular we can choose $s_0 = s_1$. Then Γ_{s_0, s_1} is a straight line $\mathbf{i}(s_0 + s_1)\mathbb{R}$. Choosing $\Re((s_0 + s_1)/|s_0 + s_1|)$ small enough yields $\mathbb{S}(\omega) \subset \Gamma_{s_0, s_1}^+$.
2. $\mathbf{i}(-\theta, 0) \cup \mathbf{i}(\theta, \infty) \subset \Gamma^+$ (Fig. 4(b)): We choose arbitrary \tilde{s}_0, \tilde{s}_1 , such that (3.12) is satisfied. E.g. we can choose \tilde{s}_0, \tilde{s}_1 as in Fig. 4(b). Then we scale $s_0 := \tilde{s}_0\theta/\zeta(\tilde{s}_0, \tilde{s}_1)$ and $s_1 := \tilde{s}_1\theta/\zeta(\tilde{s}_0, \tilde{s}_1)$, such that $\mathbf{i}\mathbb{R} \cap \Gamma_{s_0, s_1} = \{0, \pm\mathbf{i}\theta\}$. The real valued outgoing wavenumbers are now contained in $-\mathbf{i}\Gamma_{s_0, s_1}^+$. To check if the non-real outgoing wavenumbers are contained in $-\mathbf{i}\Gamma_{s_0, s_1}^+$, $g_{s_0, s_1}(\mathbf{i}\kappa_n) < 1$ can be evaluated. If not, define $s_0^t := s_0\theta/\zeta(s_0, t\bar{s}_0 + (1-t)s_1)$ and $s_1^t := (t\bar{s}_0 + (1-t)s_1)\theta/\zeta(s_0, t\bar{s}_0 + (1-t)s_1)$ for $t \in [0, 1]$. There hold $s_0^0 = s_0, s_1^0 = s_1$ and $s_0^1 = s_0, s_1^1 = \bar{s}_0$, i.e. $t \mapsto \Gamma_{s_0^t, s_1^t}$ is a homotopy between Γ_{s_0, s_1} and $\mathbf{i}\mathbb{R}$, such that $\Gamma_{s_0^t, s_1^t} \cap \mathbf{i}\mathbb{R} = \{0, \pm\mathbf{i}\theta\}$ for all $t \in [0, 1)$. Choosing $t \in [0, 1]$ close enough to one, $\mathbb{S}(\omega) \subset \Gamma_{s_0^t, s_1^t}^+$ can be ensured.

The approximation error of the method depends on $g_{s_0, s_1}(\mathbf{i}\kappa_n)^{N_{\text{long}}}$. Hence, in general one should try to find s_0 and s_1 such that $g_{s_0, s_1}(\mathbf{i}\kappa_n)$ is as small as possible for the first wavenumbers κ_n .

Note, that the wavenumbers and modes are not used in the numerical method. A rough estimate of the location of the wavenumbers is needed in

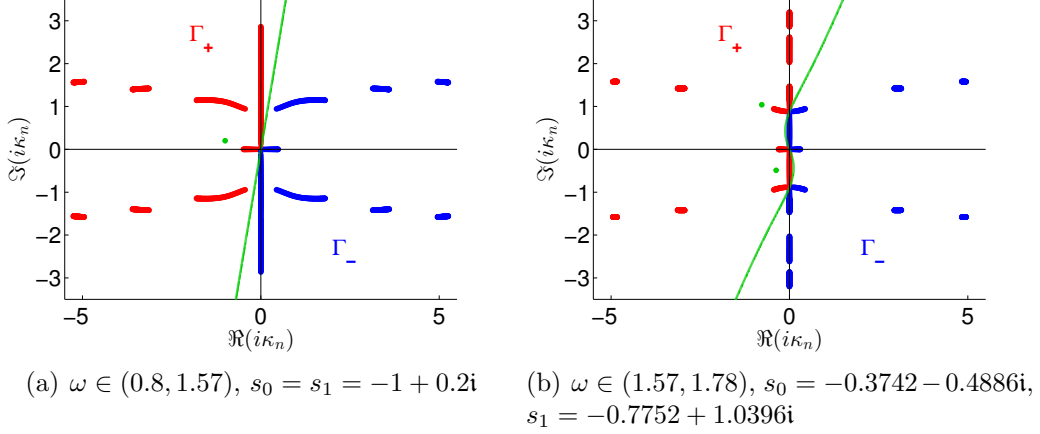


Figure 4: Lowest outgoing (red) and incoming (blue) wavenumbers (multiplied with i) for different intervals of frequencies. Separating curves Γ with parameters s_0 (and s_1) are marked green. Material parameters are $H = \rho = E = 1$ and $\nu = 0.25$.

order to choose reasonable values for s_0 and s_1 , but the Hardy space infinite element method itself is independent of the wavenumbers and the waveguide modes.

4 Tensor product discretization of one waveguide

For a discretization of (2.1) a standard finite element method for the bounded interior domain Ω_{int} can be used. For the waveguides a tensor product method appears reasonable. We present here only shortly such a tensor product method for one reference waveguide. The extension to several waveguides and the coupling with the finite element method for Ω_{int} is straightforward.

We consider again the reference waveguide $W := \mathbb{R}^+ \times (-R, R)$. For sufficiently fast decaying test functions \mathbf{v} we obtain as in the last section a variational formulation of (2.4) with the pole condition as radiation condition: We are looking for \mathbf{u} with $\mathcal{L} \mathbf{u} \in [H^-(\Gamma_{s_0, s_1}) \otimes L^2(-R, R)]^2$ such that for all suitable \mathbf{v}

$$a_{\text{ext}}(\mathbf{u}, \mathbf{v}) - \omega^2 b_{\text{ext}}(\mathbf{u}, \mathbf{v}) = - \int_{\Gamma} (\sigma(\mathbf{u}) \begin{pmatrix} 1 \\ 0 \end{pmatrix}) \cdot \mathbf{v} \, ds \quad (4.1a)$$

with $a_{\text{ext}}(\mathbf{u}^{\text{ext}}, \mathbf{v}^{\text{ext}}) := \int_W (2\mu \epsilon(\mathbf{u}) : \epsilon(\mathbf{v}) + \lambda \operatorname{div} \mathbf{u} \operatorname{div} \mathbf{v}) d(\xi, \eta)$ and $b_{\text{ext}}(\mathbf{u}, \mathbf{v}) := \int_W \rho \mathbf{u} \cdot \mathbf{v} d(\xi, \eta)$. In full detail we have

$$\begin{aligned} a_{\text{ext}}(\mathbf{u}, \mathbf{v}) &= \int_W ((2\mu + \lambda) \partial_\xi \mathbf{u}_1 \partial_\xi \mathbf{v}_1 + \mu \partial_\eta \mathbf{u}_1 \partial_\eta \mathbf{v}_1) d(\xi, \eta) + \int_W ((2\mu + \lambda) \partial_\eta \mathbf{u}_2 \partial_\eta \mathbf{v}_2 + \mu \partial_\xi \mathbf{u}_2 \partial_\xi \mathbf{v}_2) \\ &\quad + \int_W (\mu \partial_\eta \mathbf{u}_1 \partial_\xi \mathbf{v}_2 + \lambda \partial_\xi \mathbf{u}_1 \partial_\eta \mathbf{v}_2) d(\xi, \eta) + \int_W (\mu \partial_\xi \mathbf{u}_2 \partial_\eta \mathbf{v}_1 + \lambda \partial_\eta \mathbf{u}_2 \partial_\xi \mathbf{v}_1) d(\xi, \eta), \\ b_{\text{ext}}(\mathbf{u}, \mathbf{v}) &:= \int_W \rho (\mathbf{u}_1 \mathbf{v}_1 + \mathbf{u}_2 \mathbf{v}_2) d(\xi, \eta). \end{aligned}$$

The right hand side of (4.1a) cancels out with the corresponding term of the variational formulation of the interior problem, if the test functions are chosen to be continuous on the interface $\Upsilon := \{0\} \times (-R, R)$.

The whole waveguide is considered as an (in)finite element with element matrix $A^{\text{ext}} - \omega^2 B^{\text{ext}}$ and tensor product basis functions of the form $\varphi_j^{\text{long}} \otimes \varphi_l^{\text{trans}}$. More precisely, for \mathbf{u} we use the ansatz

$$\mathbf{u}(\xi, \eta) \approx \mathbf{u}_{N^{\text{long}}, N^{\text{trans}}}(\xi, \eta) := \sum_{j=1}^{N^{\text{long}}} \sum_{l=1}^{N^{\text{trans}}} \varphi_j^{\text{long}}(\xi) \varphi_l^{\text{trans}}(\eta) \begin{pmatrix} \alpha_{jl}^{(1)} \\ \alpha_{jl}^{(2)} \end{pmatrix}, \quad (\xi, \eta) \in (0, \infty) \times (-R, R) \quad (4.2)$$

with $\alpha_{jl}^{(1)}, \alpha_{jl}^{(2)} \in \mathbb{C}$.

In order to ensure continuity of the discrete solution at the interface Υ the basis functions φ_l^{trans} are the non-vanishing traces of the interior basis functions $\varphi_j^{\text{int}} \in H^1(\Omega_{\text{int}})$, i.e. for $\varphi_{j(1)}^{\text{int}}|_\Upsilon, \dots, \varphi_{j(N^{\text{trans}})}^{\text{int}}|_\Upsilon \neq 0$

$$\varphi_l^{\text{trans}}(\eta) := \varphi_{j(l)}^{\text{int}}(0, \eta), \quad \eta \in (-R, R), \quad l = 1, \dots, N^{\text{trans}}.$$

The surface matrices $M_{\text{trans}}, D_{\text{trans}}, S_{\text{trans}} \in \mathbb{C}^{N^{\text{trans}} \times N^{\text{trans}}}$ defined by

$$M_{\text{trans}} := \left(\int_{-R}^R \varphi_l^{\text{trans}} \varphi_m^{\text{trans}} d\eta \right)_{l,m=1}^{N^{\text{trans}}}, \quad D_{\text{trans}} := \left(\int_{-R}^R \partial_\eta \varphi_l^{\text{trans}} \varphi_m^{\text{trans}} d\eta \right)_{l,m=1}^{N^{\text{trans}}}, \quad S_{\text{trans}} := \left(\int_{-R}^R \rho \varphi_l^{\text{trans}} \varphi_m^{\text{trans}} d\eta \right)_{l,m=1}^{N^{\text{trans}}}, \quad (4.3)$$

can be computed e.g. by Gauss quadrature.

For the unbounded ξ -direction we use the basis functions and element matrices $M_{\text{long}}, D_{\text{long}}$ and S_{long} of the last section (we have dropped the superscripts for convenience). The system matrix of (4.1a) is therefore given by $A^{\text{ext}} - \omega^2 B^{\text{ext}} \in \mathbb{C}^{2N^{\text{long}} N^{\text{trans}} \times 2N^{\text{long}} N^{\text{trans}}}$ with

$$A^{\text{ext}} := \begin{pmatrix} (2\mu + \lambda) S_{\text{long}} \otimes M_{\text{trans}} + \mu M_{\text{long}} \otimes S_{\text{trans}} & \mu D_{\text{long}}^\top \otimes D_{\text{trans}} + \lambda D_{\text{long}} \otimes D_{\text{trans}}^\top \\ \mu D_{\text{long}} \otimes D_{\text{trans}}^\top + \lambda D_{\text{long}}^\top \otimes D_{\text{trans}} & (2\mu + \lambda) M_{\text{long}} \otimes S_{\text{trans}} + \mu S_{\text{long}} \otimes M_{\text{trans}} \end{pmatrix}, \quad (4.4a)$$

$$B^{\text{ext}} := \begin{pmatrix} \rho M_{\text{long}} \otimes M_{\text{trans}} & \mathbf{0} \\ \mathbf{0} & \rho M_{\text{long}} \otimes M_{\text{trans}} \end{pmatrix}. \quad (4.4b)$$

The coupling of the matrix $A^{\text{ext}} - \omega^2 B^{\text{ext}}$ with a system matrix $A^{\text{int}} - \omega^2 B^{\text{int}}$ of the interior problem becomes natural due to $\varphi_j^{\text{long}}(0) = \delta_{1j}$. Therefore, we have constructed an (in)finite element for each waveguide which can be easily combined with the finite element discretization of the interior problem. In more details and in 3d this construction is shown in [23, Sec. 4.1].

5 Resonance problems

Up to now, we have only considered diffraction problems. We now focus on the resonance problem (2.2). Since the modal radiation condition from Sec. 2.2 is (more or less well) defined only for positive frequencies ω , so is the resonance problem (2.2). A meaningful extension to complex valued frequencies consists in a holomorphic extension of (2.2). If $\mathbb{S}(\omega) \subset \Gamma_{s_0, s_1}^+$ holds true for all ω in a real interval (a, b) , then the pole condition (2.8) with respect to the parameters s_0, s_1 is equivalent to the modal radiation condition on this interval. Since the pole condition is independent of the frequency, it is straightforward to holomorphically extend the resonance problem from the interval (a, b) into the complex plane through the pole condition.

However, the dependence of this extension on s_0, s_1 is not obvious. The crucial property to investigate is the Fredholmness of the holomorphic extension. Due to similar results for acoustic waveguides in [15], we conjecture that the essential spectrum, i.e. the set of frequencies ω for which (2.2) equipped with the pole condition is not Fredholm, takes the form

$$\sigma_{\text{ess}}(s_0, s_1) := \{\omega \in \mathbb{C} : \mathbf{i}\kappa_n(\omega) \in \Gamma_{s_0, s_1} \text{ for all } n \in \mathbb{N}\}. \quad (5.1)$$

For complex frequencies ω the wavenumbers $\kappa_n(\omega)$ are thereby defined in the same way as for real valued frequencies, i.e. as eigenvalues of a quadratic eigenvalue problem (see Rem. 2.1). The set $\sigma_{\text{ess}}(s_0, s_1)$ can be interpreted as the union of \mathbb{N} curves, i.e. $\sigma_{\text{ess}}(s_0, s_1) = \bigcup_{n \in \mathbb{N}} \{\omega \in \mathbb{C} : \mathbf{i}\kappa_n(\omega) \in \Gamma_{s_0, s_1}\}$. Due to the point symmetry of Γ_{s_0, s_1} and of the set of wavenumbers with respect to 0, each curve starts at a frequency ω , such that there exists a vanishing wavenumber $\kappa_n(\omega) = 0$.

To support these conjectures, we give a numerical example in Fig. 5 for a waveguide $\mathbb{R} \times (-1, 1)$ with $\rho = E = 1$ and $\nu = 0.25$. For a given $\kappa \in -\mathbf{i}\Gamma_{s_0, s_1}$ the corresponding ω for which wavenumbers $\kappa_n(\omega) \in -\mathbf{i}\Gamma_{s_0, s_1}$ exist, are the square roots of a linear eigenvalue problem given in [25]. Moreover, $-\mathbf{i}\Gamma_{s_0, s_1}$ can be explicitly parameterized with $-\mathbf{i}\gamma_{s_0, s_1}$ due to (3.11). The set

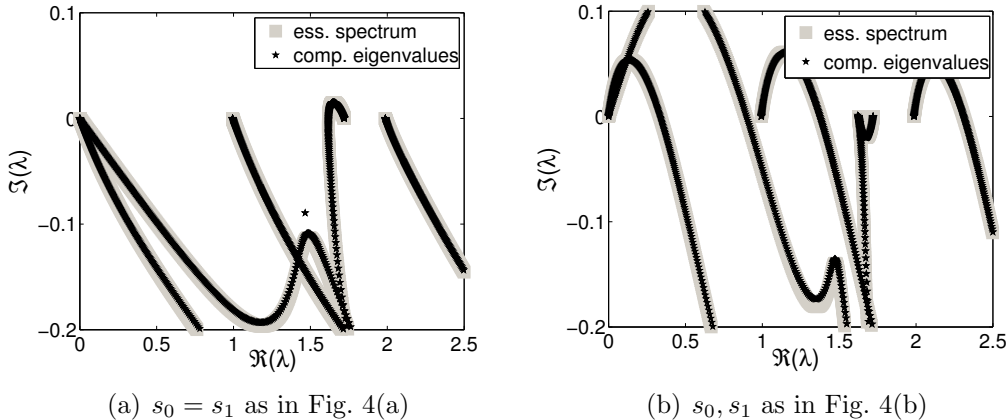


Figure 5: Eigenvalues of (2.2) for $\Omega = \mathbb{R} \times (-1, 1)$, $\rho = E = 1$ and $\nu = 0.25$ compared with the essential spectrum $\sigma_{\text{ess}}(s_0, s_1)$.

$\sigma_{\text{ess}}(s_0, s_1)$ can therefore be numerically computed with a standard eigenvalue solver. For our example we chose 1000 sample points $\kappa = -i\gamma_{s_0, s_1}(r) \in i\Gamma_{s_0, s_1}$ with equidistant $r \in (-5, 0)$ to compute $\sigma_{\text{ess}}(s_0, s_1)$. In Fig. 5 we compare it with the computed eigenvalues of (2.2), where we used a high order finite element method for $\Omega_{\text{int}} = (0, 5) \times (-1, 1)$ with a triangular mesh with maximal meshwidth $h = 0.1$ and polynomial order $p = 12$. The two waveguides $(5, \infty) \times (-1, 1)$ and $(-\infty, 0) \times (-1, 1)$ are discretized using Hardy space infinite elements with $N^{\text{long}} = 200$. For the generalized linear eigenvalue problem we have used a shift-and-invert Arnoldi algorithm with four different shifts and a Krylov space with dimension 2000.

It can be seen in Fig. 5 that almost all of the computed eigenvalues $\lambda \in \mathbb{C}$ fit very well to $\sigma_{\text{ess}}(s_0, s_1)$. Thus their interpretation as the discretization of an essential spectrum is reasonable. The isolated point in Fig. 5(a) has to be interpreted as a resonance. We clearly see in Fig. 5 that different parameter choices s_0, s_1 lead to different essential spectra, as predicted through $\sigma_{\text{ess}}(s_0, s_1)$. We also observe a dependence of the discrete spectrum on the parameters. This is because the different parameters correspond to different choices of branches of the solution operator. This behavior will be discussed in more detail in Sec. 6.3.

Moreover, we observe in Fig. 5 that some curves of the essential spectrum are partially located in the quadrant $\{z \in \mathbb{C} : \Re(z), \Im(z) > 0\}$. Each such curve admits in addition to its starting point a supplementary intersection ω^* with the real axis. This means that there exists a wavenumber $\kappa_n(\omega)$ crossing over $-i\Gamma_{s_0, s_1}$ as ω moves along the real interval $(\omega^* - \epsilon, \omega^* + \epsilon)$

(for some $\epsilon > 0$). Since the pole condition selects wavenumbers in $-\mathbf{i}\Gamma_{s_0, s_1}^+$, it can't be equivalent to the modal radiation condition for both intervals $(\omega^* - \epsilon, \omega^*)$, $(\omega^*, \omega^* + \epsilon)$ simultaneously. A inspection of such cases shows, that for intervals I with $\sigma_{\text{ess}}(s_0, s_1) \cap \{x + \mathbf{i}y: x \in I, y > 0\} \neq \emptyset$ the pole condition is never equivalent to the modal radiation condition. Note, that such an interval exists in Fig. 5(a) indicating the presence of a backward propagating mode for $\omega \in (1.58, 1.65)$ (compare with Fig. 3). Since the Hardy space infinite element method only depends on s_0 and s_1 , for this finding no calculation of wavenumbers or waveguide modes was needed.

It is worth mentioning that the discrete and essential spectra can also be interpreted in terms of the solution operator to (2.2) with respect to the pole condition. Resonances correspond to poles and the essential spectrum corresponds to branch cuts of the solution operator.

We conclude, that the computed eigenvalues of (2.2) have to be interpreted carefully. They might be part of the discretization of an essential spectrum. If this is not the case, they are approximations to the resonances of (2.2). These resonances depend on the parameter choice and belong to different Riemann sheets. The relevance of resonances for scattering problems will be investigated further in Sec. 6.2 Note, that the discretization of (2.2) with Hardy space infinite elements leads to a generalized linear eigenvalue problem, which can be solved using a standard linear eigenvalue solver. This is one of the advantages of the presented method over classical modal methods.

6 Numerical results

Since rigorous convergence results are not available for Hardy space elements in the context of elastic waveguide problems, we report here on numerical experiments. The convergence results for acoustic waveguide problems in [15] and of the model problem in [13] indicate a super-algebraic convergence rate with respect to the number of unknowns in the infinite direction. The first numerical experiment for a diffraction problem with a known solution supports this conjecture. The second numerical experiment underlines the relation between a scattering problem and the corresponding resonance problem. The last experiment illustrates the dependency of the computed resonances on the method parameters.

The computations were all made with the finite element package netgen/NGSolve [26, 27] and the module ngs-waves [24] containing the source code for Hardy space methods. For the resonance problems we have used a standard shift-and-invert Arnoldi method using MUMPS or PARDISO as

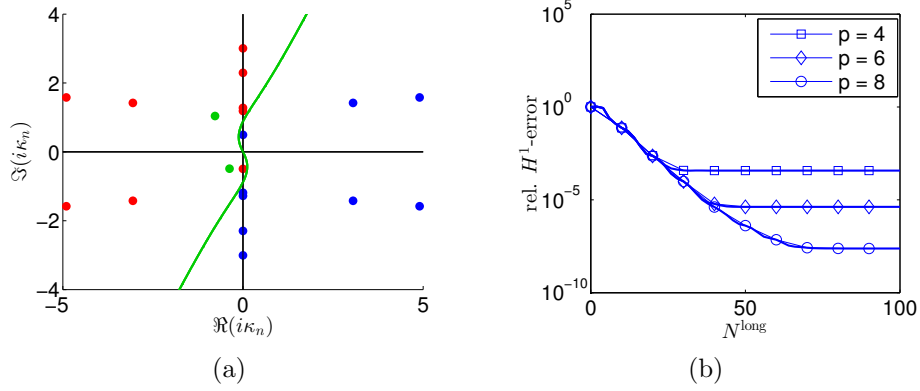


Figure 6: Left panel: outgoing (red) and incoming (blue) $i\kappa_n$ for $\omega = 1.66$. Right panel: relative $(H^1(\Omega_{\text{int}}))^2$ -error of $\mathbf{u} - \mathbf{u}_{\text{ref}}$ w.r.t. the number of unknowns N^{long} in the infinite direction for different polynomial orders.

direct solver.

6.1 Convergence test

For unperturbed waveguides $W = \mathbb{R}^+ \times (-R, R)$ the Rayleigh-Lamb modes are known to be (semi-)explicit solutions to (2.4) (see e.g. [2]): We define the longitudinal wave speed by $c_L := \sqrt{(\lambda + 2\mu)/\rho}$, the transversal wave speed by $c_T := \sqrt{\mu/\rho}$, and for $\kappa \in \mathbb{C}$ the dispersion relations

$$F_S(\kappa) := 4\kappa^2\alpha\beta \sin(\alpha R) \cos(\beta R) + (\kappa^2 - \beta^2)^2 \cos(\alpha R) \sin(\beta R), \quad (6.1a)$$

$$F_A(\kappa) := 4\kappa^2\alpha\beta \cos(\alpha R) \sin(\beta R) + (\kappa^2 - \beta^2)^2 \sin(\alpha R) \cos(\beta R), \quad (6.1b)$$

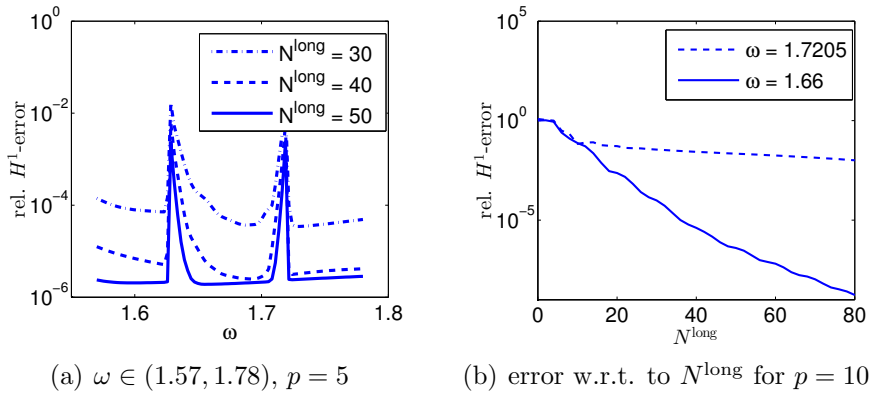


Figure 7: relative $(H^1(\Omega_{\text{int}}))^2$ -error of $\mathbf{u} - \mathbf{u}_{\text{ref}}$ for different frequencies ω

with $\alpha := \sqrt{\omega^2/c_L^2 - \kappa^2}$ and $\beta := \sqrt{\omega^2/c_T^2 - \kappa^2}$. If κ is a root of $F_S(\kappa) = 0$ or $F_A(\kappa) = 0$, then

$$\mathbf{u}^S(\xi, \eta) := e^{i\kappa\xi} \mathbf{w}^S(\eta), \quad \mathbf{u}^A(\xi, \eta) := e^{i\kappa\xi} \mathbf{w}^A(\eta), \quad (\xi, \eta) \in W,$$

with

$$\mathbf{w}^S(\eta) := \begin{pmatrix} i\kappa(\kappa^2 - \beta^2)^2 \sin(\beta R) \cos(\alpha\eta) + \beta 2i\kappa\alpha \sin(\alpha R) \cos(\beta\eta) \\ -\alpha(\kappa^2 - \beta^2)^2 \sin(\beta R) \sin(\alpha\eta) + 2\kappa^2\alpha \sin(\alpha R) \sin(\beta\eta) \end{pmatrix}, \quad (6.2a)$$

$$\mathbf{w}^A(\eta) := \begin{pmatrix} i\kappa(\kappa^2 - \beta^2)^2 \cos(\beta R) \sin(\alpha\eta) - \beta 2i\kappa\alpha \cos(\alpha R) \sin(\beta\eta) \\ \alpha(\kappa^2 - \beta^2)^2 \cos(\beta R) \cos(\alpha\eta) + 2\kappa^2\alpha \cos(\alpha R) \cos(\beta\eta) \end{pmatrix}, \quad (6.2b)$$

are the symmetric and anti-symmetric Rayleigh-Lamb modes.

We chose for $R = 1$, Young's modulus $E = 1$, density $\rho = 1$ and Poisson's ratio $\nu = 0.25$ the reference function

$$\mathbf{u}_{\text{ref}} := \sum_{j=1}^5 \mathbf{u}_j^S / \|\mathbf{w}_j^S\|_{L^2(\Upsilon)} + \sum_{j=1}^4 \mathbf{u}_j^A / \|\mathbf{w}_j^A\|_{L^2(\Upsilon)} \quad (6.3)$$

with the first five symmetric and first four anti-symmetric Rayleigh-Lamb modes. The domain is given by $\Omega = \Omega_{\text{int}} \cup \Upsilon \cup W$ with $\Omega_{\text{int}} = (0, 15) \times (-1, 1)$ triangulated with maximal mesh size $h = 0.25$, $\Upsilon = \{15\} \times (-1, 1)$, and $W = (15, \infty) \times (-1, 1)$. (2.4) was completed with the Dirichlet boundary condition $\mathbf{u}(0, \bullet) = \mathbf{u}_{\text{ref}}(0, \bullet)$ and the pole condition (2.8) for Γ_{s_0, s_1} defined in Sec. 3.2 with $s_0 = -0.374158 - 0.488609i$ and $s_1 = -0.775234 + 1.03962i$.

First we pick a fixed frequency $\omega = 1.66$, such that there exists an outgoing wavenumber $\kappa(\omega) < 0$ (see Fig. 6(a)) and vary the polynomial order of the finite element method for Ω_{int} and the number of unknowns N^{long} in the infinite direction (see Fig. 6(b)). Super-algebraic convergence in N^{long} can be observed until the error of the finite element discretization of the interior problem, which depends on the polynomial order, is reached.

In Fig. 7(a) we fixed the uniform polynomial degree to $p = 5$ and varied $\omega \in (1.57, 1.78)$. At the frequencies $\omega \approx 1.6260, \omega \approx 1.7206$ the method fails, as already mentioned in Sec. 3.3, since for these frequencies one outgoing wavenumber coincides with an incoming one. Apart from these frequencies, the relative error in Ω_{int} is small. But if we chose $\omega = 1.7205$ such that there exists one wavenumber $\kappa_n \approx 0$, the convergence rate w.r.t. N^{long} is very poor (see 7(b) with $p = 10$). Techniques to overcome this problem were developed for acoustic waveguide problems in [15]. The application to elastic waveguide problems is intended for future research.

6.2 Cavity resonances

We consider a waveguide $\mathbb{R} \times (-1, 1)$ with a cavity $\Omega_1 := (-5, 5) \times [1, 6)$ attached to some wall at the homogeneous Dirichlet-boundary $\partial\Omega_D = (-5, 5) \times$

$\{6\}$. On all other parts of the boundary we assume homogeneous Neumann boundary conditions. In Fig. 8(a) the triangulation of the interior domain $\Omega_{\text{int}} = (-10, 10) \times (-1, 1) \cup \Omega_1$ is given.

First, we have solved scattering problem (2.1) for different frequencies $\omega \in (1.58, 1.65)$ with an incoming wave consisting of propagating Lamb modes and measured the stress in the cavity Ω_1 , which is plotted in Fig. 8(b). We have chosen the material parameters as in the last subsection, in order to ensure the existence of backward propagating modes in the stated frequency interval.

Second, we solve the resonance problem (2.2) for the same material parameters and look for resonances near the interval $(1.58, 1.65)$. In Fig. 9 the computed eigenvalues for two different pairs of s_0 and s_1 are given. We can detect in Fig. 9 four eigenvalues, are separated from the remaining spectrum. They are $\omega_1 = 1.609 - 0.019i$, $\omega_2 = 1.625 - 0.003i$, $\omega_3 = 1.655 - 0.003i$, and $\omega_4 = 1.66 - 0.011i$. Moreover these eigenvalues coincide for both calculations obtained with different method parameters. Since the essential spectrum depends on the method parameters, we can identify them as resonances.

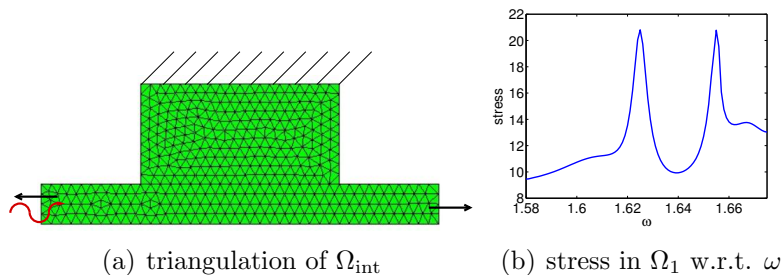


Figure 8: scattering of a wave signal by a cavity with Dirichlet boundary conditions

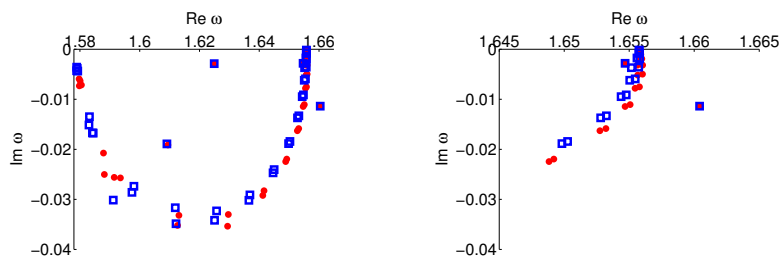


Figure 9: The computed spectrum for a pair of parameters s_0, s_1 indicated as red points, and for a slightly perturbed pair \tilde{s}_0, \tilde{s}_1 indicated as blue squares. The right plot is a magnification of one part of the left plot.

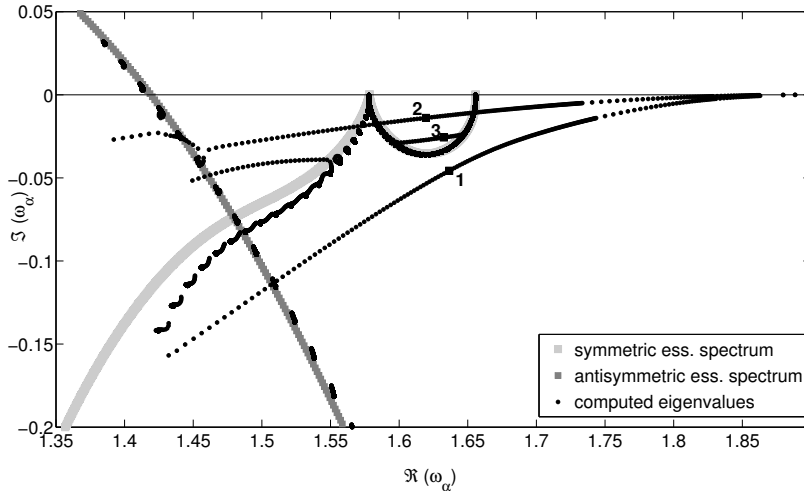


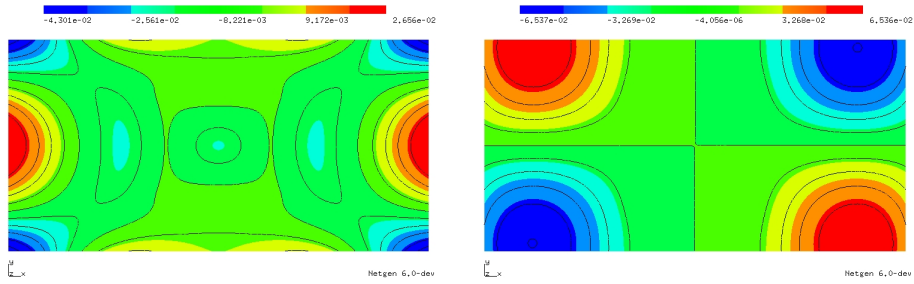
Figure 10: the computed spectrum for $s_0 = -0.182086 - 0.237784i$, $s_1 = -1.71492 + 2.29978i$ and varying $\alpha \in (5, 10^{10})$; eigenvalues near to shaded domains are discretizations of two curves $\{\omega \in \mathbb{C} : i\kappa_n(\omega) \in \Gamma_{s_0, s_1}\}$ of the essential spectrum (see Sec. 5) with κ_n being the wavenumbers to one anti-symmetric Lamb mode and to one symmetric, backward propagating Lamb mode. The squares indicate the resonances for $\alpha = 11$.

If we compare Fig. 8(b) with Fig. 9, we observe that the two peaks in Fig. 8(b) fit very well to the two computed resonances ω_{res} from Fig. 9 with $|\Im(\omega_{\text{res}})|$ most low, i.e. ω_2 and ω_3 . This is not surprising, since apart from the essential spectrum we expect the solution operator to be meromorphic with respect to the frequency with resonances being the poles. Hence, in the neighborhood of a resonance the scattering problem is almost singular and thus very sensitive to external forces.

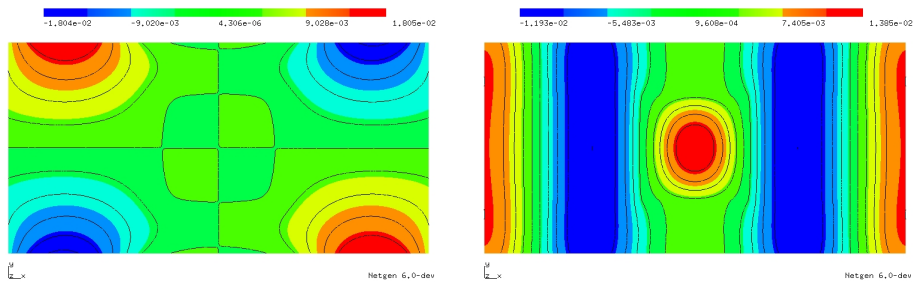
6.3 Dependency of resonances with respect to s_0, s_1

In this subsection we want to highlight that the choice of the parameters s_0, s_1 for solving a resonance problem corresponds to a choice of the Riemann sheet on which resonances are sought. We construct an example problem parameterized by a parameter $\alpha \in \mathbb{R}^+$, such that we have some a priori knowledge about the resonances and observe the influence of the choice of Riemann sheets on the resonances.

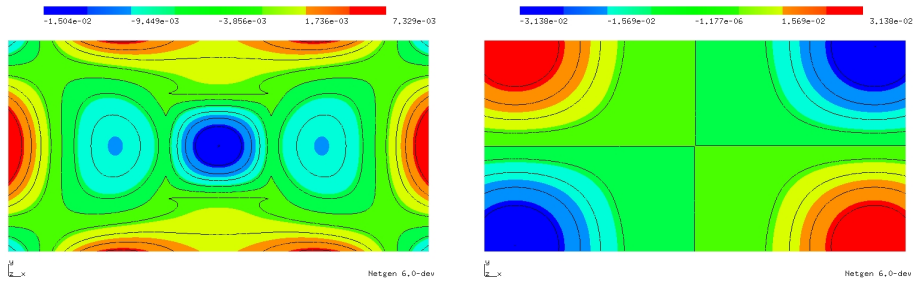
We are solving (2.2) for $\Omega = \mathbb{R} \times (-1, 1)$ with density $\rho = 4$ for $\mathbf{x} \in \Omega_1 := [-0.5, 0.5]^2$ and $\rho = 1$ elsewhere, Young's modulus $E = 1$ and Poisson's ratio $\nu = 0.2$ and $\mathcal{B}\mathbf{u} := \sigma(\mathbf{u}) \cdot \mathbf{n}$. Moreover, we added to (2.2) a jump in the



(a) resonance 1 in Fig. 10 ($\omega \approx 1.636 - 0.045i$)



(b) resonance 2 in Fig. 10 ($\omega \approx 1.620 - 0.014i$)



(c) resonance 3 in Fig. 10 ($\omega \approx 1.633 - 0.026i$)

Figure 11: real part of first (left panels) and second (right panels) Cartesian component of a resonance function for $\alpha = 11$.

normal stress on $\partial\Omega_1$

$$(\sigma(\mathbf{u}^+) - \sigma(\mathbf{u}^-)) \cdot \mathbf{n} = \alpha \mathbf{u} \quad \text{for } \mathbf{x} \in \partial\Omega_1, \quad \alpha \in \mathbb{C},$$

leading to an additional term $\alpha \int_{\partial\Omega_1} \mathbf{u}^{\text{int}} \cdot \mathbf{v}^{\text{int}} ds$.

For the discretization we have used a high order finite element method for $\Omega_{\text{int}} = (-2, 2) \times (-1, 1)$ based on a triangulation with maximal meshsize $h = 0.1$ and a finite element order 10. The waveguides are discretized using the Hardy space infinite elements with 150 basis functions in $H^-(\Gamma_{s_0, s_1})$ and $s_0 = -0.182086 - 0.237784i$, $s_1 = -1.71492 + 2.29978i$. Since there exists a backward propagating mode (see Fig. 2 for $\omega = 1.615$), the parameters are chosen such that the pole condition is equivalent to the modal radiation condition in the neighborhood of 1.615.

For $\alpha \rightarrow \infty$ the additional term leads to two decoupled problems for Ω_1 and $\Omega \setminus \Omega_1$ with Dirichlet boundary conditions at $\partial\Omega_1$. Hence, for $\alpha \rightarrow \infty$ some of the resonances ω_α should converge to the square root of the (real) Dirichlet-eigenvalues of the problem in the bounded domain Ω_1 , which can be computed using standard finite element methods. This can be observed in Fig. 10: The sequences of resonances labeled with 1 and 2 are converging for $\alpha \rightarrow \infty$ to ≈ 1.89 , which is the square root of a real eigenvalue with geometric multiplicity 2.

In order to distinguish resonances from discretizations of the essential spectrum, we have computed as in Sec. 5 additionally the essential spectrum of the resonance problem, which depends on s_0 and s_1 . For $\alpha = 11$ the real part of the Cartesian components of three resonance functions can be seen in Fig. 11. We notice that resonances labeled with 1 have symmetric resonance functions (as well as these labeled with 3) and the resonances labeled with 2 have antisymmetric resonance functions.

In order to illustrate the effect of the essential spectrum on the resonance functions, we have computed first for the sequence 2 of resonances $\omega_\alpha^{(2)}$ in Fig. 12 the wavenumbers $\kappa_n(\omega_\alpha^{(2)})$ multiplied with i . The Hardy space method computes resonance functions with wavenumbers in $-i\Gamma_+$. Since for two sequences of symmetric wavenumbers there exists an intersection with Γ and therefore jumps in these wavenumbers, we would expect jumps in the resonances $\omega_\alpha^{(2)}$, too. These jumps would be in Fig. 10 exactly at the intersection points of $\omega_\alpha^{(2)}$ with the essential spectrum. Since the resonance functions corresponding to $\omega_\alpha^{(2)}$ are purely antisymmetric, they are orthogonal to the symmetric Lamb waves and thus not influenced by the change of symmetric wavenumbers. Therefore the resonances labeled with 2 are crossing in Fig. 10 the curve of the essential spectrum corresponding to a symmetric Lamb mode without any perturbation but stop at the curve of the essential spectrum cor-

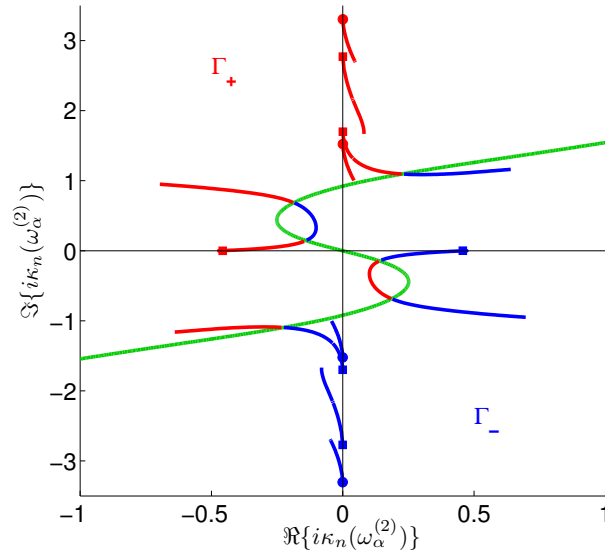
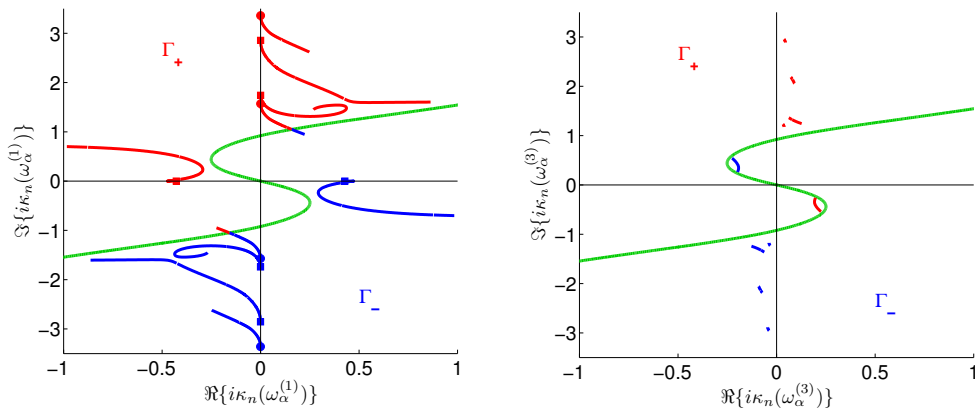


Figure 12: wavenumbers (multiplied with i) for the complex resonances 2 of Fig. 10 with $\alpha \in (6, 10^{10})$ computed with [25]. The squares indicate the wavenumbers for $\alpha = 10^{10}$ of the symmetric Lamb waves, circles of the antisymmetric Lamb waves. The parameters for the green curve Γ_{s_0, s_1} are the same as in Fig. 10.

responding to an antisymmetric Lamb mode. The last statement can be also seen in Fig. 12, since for $\alpha \approx 6$ one antisymmetric wavenumber hits Γ .

Fig. 13 shows similar results for the resonances labeled with 1 and 3, where the resonance functions are both symmetric. E.g. the resonances $\omega_\alpha^{(3)}$ seem to vanish after reaching the essential spectrum corresponding to a symmetric Lamb mode. The resonances 1 are the counterparts of the resonances 3 on a different Riemann sheet: For $\alpha = 11$ both resonances are present and belong to the same Riemann sheet, which is determined by the chosen parameters s_0 and s_1 . The modal radiation condition of Sec. 2.2 for the real parts $\Re\{\omega_{11}^{(1)}\}$ and $\Re\{\omega_{11}^{(3)}\}$ of the resonances support a backward propagating mode (for the real parts of the resonances see Fig. 10, the corresponding dispersion curves are given in Fig. 2(a)). $\omega_{11}^{(3)}$ is located above and $\omega_{11}^{(1)}$ below the essential spectrum arising from a branch cut of the holomorphic extension of this backward propagating mode. For $\alpha \approx 11.7$ the resonances $\omega_\alpha^{(3)}$ hit the branch cut and vanish with increasing α , since the Riemann sheet of their existence is hidden in this part of the complex plane. Hence, for larger values of α we can see in Fig. 10 only the resonances $\omega_\alpha^{(1)}$.



(a) $\alpha \in (5, 10^{10})$. The squares indicate the wavenumbers for $\alpha = 10^{10}$ of the symmetric Lamb waves, circles of the antisymmetric Lamb waves

(b) $\alpha \in (9.4, 11.7)$

Figure 13: wavenumbers (multiplied with i) for the complex resonances 1 (left) and 3 (right) of Fig. 10 w.r.t. α computed with [25]. The parameters for the green curve Γ_{s_0, s_1} are the same as in Fig. 10.

7 Conclusion

In this paper we addressed the topic of backward propagating modes in time-harmonic two-dimensional elastic waveguides. The so called pole condition allows to reformulate the radiation condition even in the presence of backward waves without using the waveguide modes or wavenumbers. For the problems under consideration a special class of pole conditions depending on two complex parameters s_0 and s_1 is sufficient. Detailed explanations on the choice of these parameters are given in Section 3.3. The Hardy space infinite element method developed in [13] relies on this pole condition and can be easily applied to waveguide structures using tensor product elements.

An outstanding property of the presented scheme is that it is independent of the waveguide modes and wavenumbers which simplifies the implementation. Moreover, a discretization of a resonance problem leads to a generalized linear matrix eigenvalue problem, which is much easier to handle than a non-linear problem. However, the interpretation of the occurring spectral objects for resonance problems is rather involved and was addressed in Section 5 and Section 6.3.

The method shows in numerical examples super-algebraic convergence for diffraction problems. For resonance problems the numerical results also coincide with the theoretical considerations. In particular, a strong relation between the resonances and the behavior of the solutions to diffraction problems with frequencies in the neighborhood of a resonance frequency can be seen. Hence, resonance and diffraction problems in two dimensional waveguides can be reliably solved using the Hardy space infinite element method.

References

- [1] S. ABARBANEL, D. GOTTLIEB, AND J. HESTHAVEN, *Well-posed perfectly matched layers for advective acoustics*, Journal of Computational Physics, 154 (1999), pp. 266 – 283.
- [2] J. D. ACHENBACH, *Wave Propagation in Elastic Solids (North-Holland Series in Applied Mathematics and Mechanics)*, North-Holland series in applied mathematics and mechanics, v. 16, North Holland, 1987.
- [3] V. BARONIAN, A.-S. BONNET-BENDHIA, AND E. LUNÉVILLE, *Transparent boundary conditions for the harmonic diffraction problem in an elastic waveguide*, Journal of Computational and Applied Mathematics, 234 (2010), pp. 1945–1952.
- [4] É. BÉCACHE, A.-S. BONNET-BENDHIA, AND G. LEGENDRE, *Perfectly matched layers for the convected Helmholtz equation*, SIAM Journal on Numerical Analysis, 42 (2004), pp. 409–433.
- [5] E. BÉCACHE, S. FAUQUEUX, AND P. JOLY, *Stability of perfectly matched layers, group velocities and anisotropic waves*, J. Comput. Phys., 188 (2003), pp. 399–433.
- [6] J.-P. BERENGER, *A perfectly matched layer for the absorption of electromagnetic waves*, J. Comput. Phys., 114 (1994), pp. 185–200.
- [7] W.-J. BEYN, *An integral method for solving nonlinear eigenvalue problems*, Linear Algebra and its Applications, 436 (2012), pp. 3839 – 3863. Special Issue dedicated to Heinrich Voss’s 65th birthday.
- [8] A.-S. BONNET-BENDHIA, C. CHAMBEYRON, AND G. LEGENDRE, *On the use of perfectly matched layers in the presence of long or backward guided elastic waves*, Wave Motion, (to appear).
- [9] D. BRAESS, *Finite Elemente*, Springer, 2003.

- [10] D. E. CHIMENTI, *Guided waves in plates and their use in materials characterization*, Applied Mechanics Reviews, 50 (1997), pp. 247–284.
- [11] D. GIVOLI, *High-order local non-reflecting boundary conditions: a review*, Wave Motion, 39 (2004), pp. 319–326.
- [12] K. GRAFF, *Wave Motion in Elastic Solids*, Oxford engineering science series, Clarendon Press, 1975.
- [13] M. HALLA, T. HOHAGE, L. NANNEN, AND J. SCHÖBERL, *Hardy space infinite elements for time-harmonic wave equations with phase velocities of different signs*, preprint, Institute for Analysis and Scientific Computing, TU Wien, 2014.
- [14] T. HOHAGE AND L. NANNEN, *Hardy space infinite elements for scattering and resonance problems*, SIAM J. Numer. Anal., 47 (2009), pp. 972–996.
- [15] ———, *Convergence of infinite element methods for scalar waveguide problems*, BIT Numerical Mathematics, 55 (2015), pp. 215–254.
- [16] T. HOHAGE, F. SCHMIDT, AND L. ZSCHIEDRICH, *Solving time-harmonic scattering problems based on the pole condition. I. Theory*, SIAM J. Math. Anal., 35 (2003), pp. 183–210.
- [17] A. G. KOSTYUCHENKO AND M. B. ORAZOV, *Problem of oscillations of an elastic half cylinder and related self-adjoint quadratic pencils*, Journal of Soviet Mathematics, 33 (1986), pp. 1025–1065.
- [18] H. LAMB, *On group - velocity*, Proceedings of the London Mathematical Society, s2-1 (1904), pp. 473–479.
- [19] K.-J. LANGENBERG, R. MARKLEIN, AND K. MAYER, *Ultrasonic Non-destructive Testing of Materials*, CRC Press, feb 2012.
- [20] M. LEVITIN AND M. MARLETTA, *A simple method of calculating eigenvalues and resonances in domains with infinite regular ends*, Proc. Roy. Soc. Edinburgh Sect. A, 138 (2008), pp. 1043–1065.
- [21] M. J. LIGHTHILL, *Group velocity*, J. Inst. Math. Appl., 1 (1965), pp. 1–28.
- [22] L. MTIVIER, R. BROSSIER, S. LABB, S. OPERTO, AND J. VIRIEUX, *A robust absorbing layer method for anisotropic seismic wave modeling*, Journal of Computational Physics, 279 (2014), pp. 218 – 240.

- [23] L. NANNEN, T. HOHAGE, A. SCHÄDLE, AND J. SCHÖBERL, *Exact Sequences of High Order Hardy Space Infinite Elements for Exterior Maxwell Problems*, SIAM J. Sci. Comput., 35 (2013), pp. A1024–A1048.
- [24] L. NANNEN AND J. SCHÖBERL, *Software module ngs-waves*. <http://sourceforge.net/projects/ngs-waves/>, 2014. addon to the mesh generator Netgen and the high order finite element code NGSolve.
- [25] V. PAGNEUX AND A. MAUREL, *Determination of lamb mode eigenvalues*, The Journal of the Acoustical Society of America, 110 (2001), pp. 1307–1314.
- [26] J. SCHÖBERL, *Netgen - an advancing front 2d/3d-mesh generator based on abstract rules*, Comput.Visual.Sci, 1 (1997), pp. 41–52.
- [27] —, *C++11 implementation of finite elements in ngsolve*, Preprint 30/2014, Institute for Analysis and Scientific Computing, TU Wien, 2014.
- [28] E. A. SKELTON, S. D. M. ADAMS, AND R. V. CRASTER, *Guided elastic waves and perfectly matched layers*, Wave Motion, 44 (2007), pp. 573–592.
- [29] J. TAGO, L. MTIVIER, AND J. VIRIEUX, *Smart layers: a simple and robust alternative to pml approaches for elastodynamics*, Geophysical Journal International, 199 (2014), pp. 700–706.